CARBON 53 (2013) 81–89

Available at www.sciencedirect.com

SciVerse ScienceDirect

journal homepage: www.elsevier.com/locate/carbon

Excimer laser reduction and patterning of graphite oxide

Denis A. Sokolov [a], *Christopher M. Rouleau* [c], *David B. Geohegan* [c], *Thomas M. Orlando* [a,b,*]

[a] *Georgia Institute of Technology, School of Chemistry and Biochemistry, 901 Atlantic Drive NW, Atlanta, GA 30332-0400, USA*
[b] *Georgia Institute of Technology, School of Physics, 837 State Street, Atlanta, GA 30332-0430, USA*
[c] *Center for Nanophase Materials Sciences, Oak Ridge National Laboratory, 1 Bethel Valley Road, Oak Ridge, TN 37831-6488, USA*

ARTICLE INFO

Article history:
Received 31 July 2012
Accepted 15 October 2012
Available online 23 October 2012

ABSTRACT

A successful approach and the operational parameters necessary for reduction of graphite oxide (GO) to multilayer graphene using 248 nm excimer laser irradiation in both vacuum and ultrahigh purity N_2 background environments is described. The utility of excimer laser reduction is demonstrated by production of simple line and logo patterns using standard microscale lithographic patterning strategies. Multilayer graphene formation is confirmed with Raman and X-ray photoelectron spectroscopies, and the morphology of the processed GO sample is evaluated with scanning electron microscopy. Four-point probe measurements of the excimer laser reduced GO indicate typical sheet resistances of ~100–500 Ω/sq, which is a significant improvement over other values reported in the literature for other laser-based GO reduction methods.

1. Introduction

Over the past several years, graphene has attracted significant interest from the global research community due to its combination of high electrical and thermal conductivities, high transparency, and unparalleled sheet strength, promising new solutions for applications such as transparent conductive electrodes in flexible electronics. Thus, much effort has been dedicated to the topic of graphene production. The typical methods for producing graphene include exfoliation of graphite [1], epitaxial growth on silicon carbide via silicon sublimation [2], chemical vapor deposition growth on metals from carbon precursors [3], and the reduction of graphite oxide (GO) [4–16].

To date, many GO reduction schemes have been proposed, and these can be categorized in three broad categories: thermal reduction [4,5,17], chemical reduction [6,7] and photoreduction [8,16]. More recently, several research groups have been investigating a laser approach for the photoreduction of GO [10–15]. Even though many GO reduction methods have been reported so far, very few groups have demonstrated definitive graphene formation from GO as verified by observation of the characteristic G′ peak in the Raman spectra [4,14,16] and a corresponding low sheet resistance. Laser reduction approaches that rely upon the use of inert background gas have been shown to achieve the best reduction of graphite oxide as verified with Raman spectroscopy [14]. The roles of the inert gas and plasma plume interactions in laser reduction of GO are not well understood. Most laser-based approaches implicate purely thermal processes as the primary reduction pathways. Though thermal and chemical reduction produces graphene with significant defects, the combination of these two reduction strategies decreases the net defect densities [4]. However, it is difficult to carry out these combined strategies in the spatially controlled manner needed for device fabrication.

Pulsed excimer lasers have been enabling tools at the forefront of laser processing that includes state-of-the-art lithographic nanopatterning, where their deep ultraviolet (UV) wavelengths, coupled with new interferometric techniques,

* *Corresponding author:* Fax: +1 404 3856057.
E-mail address: Thomas.Orlando@chemistry.gatech.edu (T.M. Orlando).
0008-6223/$ - see front matter
http://dx.doi.org/10.1016/j.carbon.2012.10.034

[18] have overcome previous concepts of optical lithography limitations to routinely allow the fabrication of feature sizes well below 100 nm [19,20]. In the present case, the strong laser-induced electric fields and deep ultraviolet (UV) wavelengths can provide electronic excitation and non-thermal desorption pathways as well. In fact, our previous work [14] indicated that graphite-oxide reduction was improved using 355 nm photons instead of 532 nm photons due to more efficient optical coupling. Since fully oxidized GO has a strong absorbance at 5.37 eV (231 nm) [21], it was natural to extend the process to 4.99 eV (248 nm).

In this paper, we employ 248 nm excimer laser light to examine the role of pulsed deep-UV reduction of GO. Micro-Raman spectra, X-ray photoelectron spectroscopy (XPS) spectra, laser-shot and power dependence data are presented in Section 3. These results collectively demonstrate that the use of a high purity inert background gas or a vacuum environment in conjunction with the appropriate number of incubation laser pulses is the key to successful laser reduction of graphite oxide. We determine that the very low oxygen content (~2–4%) on/in the graphene lattice produced via laser irradiation of GO results in a minimal disruption of the graphene structure. We briefly discuss the mechanisms and the potential utility of this approach in device fabrication strategies. We demonstrate that the merging of the well-established excimer laser lithographic techniques with our approach for GO reduction allows microscale patterning and will allow fabrication of graphene features with nanoscale resolution in the near future.

2. Experimental

2.1. Materials

Graphite oxide was synthesized using a modified Hummers' method [22,23] (the reaction time was increased to 7 days to allow for a complete oxidation of graphite) and was purified via dilution with nanopure water followed by centrifugation. The purification procedure was repeated until the solution reached pH 7. The graphite oxide solution was then concentrated using centrifugation and was stored in a brown glass container to prevent exposure to light. The stock solution concentration (~3.115 mg mL^{-1}) was determined by weighing a dried GO film produced from a known volume of the concentrated GO solution. Thick GO films were produced with a 47 mm diameter high pressure filtration funnel (Pall Corporation). The thickness of the produced films depends on the concentration of the graphite oxide solution. For these experiments 5 mL of concentrated GO solution was pipetted out and mixed with enough deionized water to make a 50 mL solution. The solution was pressure-filtered through a Whatman 47 mm nylon filter membrane with 200 nm pores at 170 psi of head pressure. The filtered graphite oxide on the nylon membrane was dried for 24 h at 105 °C in an oven to produce uniformly thick free standing GO films. These films were approximately 5–8 μm thick and were stored in a dessicator prior to being used.

It is necessary to clarify that in the literature there appears to be a wide discrepancy as to the exact amount of oxygen present in GO. We believe that variations arise because of the drying and storage procedures utilized in the various experiments. In our work, by following the experimental procedure outlined above, the starting GO films always contained identical amounts of oxygen (~29%) as determined by XPS analysis (the typical XPS detection limit ranges between 0.05 and 0.1 atomic percent for all elements). Due to the ease of GO partial photo- and thermal reduction, it is necessary to protect both the solution and dried powder from exposure to ambient light and temperatures in excess of 105 °C.

2.2. Graphite oxide reduction

The laser reduction experiments performed at the Center for Nanophase Materials Sciences (Oak Ridge National Laboratory) utilized a Lambda Physik LPX-300 KrF excimer laser (25 ns pulse width) with an excitation wavelength of 248 nm. A 10×10 mm aperture was imaged onto the sample at approximately 5:1 reduction using a projection beamline, and produced a rectangular spot on the GO sample that was $\sim 1.8 \times 1.98$ mm. The sample was mounted in the vacuum chamber equipped with XY translation. The laser was operated at a repetition rate of 1 Hz, and an attenuator was used to achieve laser fluences that ranged from 60 mJ cm^{-2} to 400 mJ cm^{-2}. For sheet resistance measurements, a similar excimer laser setup was utilized at the Georgia Institute of Technology that produced larger spot sizes.

Three experimental conditions were employed to promote a reducing environment: high vacuum ($\sim 10^{-6}$ Torr), low vacuum (9.8×10^{-2} Torr), and flowing (500 sccm) ultrahigh purity N_2.

2.3. Material characterization

Raman spectra were acquired with a Bruker Senterra micro-Raman spectrometer (9 cm^{-1} spectral resolution) using a 532 nm excitation wavelength and a 20× objective (Olympus M Plan 20×/0.40 ∞/0). Micro-Raman mapping was performed through a 100× objective (Olympus M Plan 100×/0.90 ∞/0). The laser power was attenuated to 2 mW to prevent sample damage due to laser heating. XPS spectra were collected with a Thermo Scientific K-Alpha XPS system using an Al Ka X-ray source. The spot size of the X-ray beam was set to 200 μm. Scanning electron microscopy (SEM) images were acquired using a Zeiss Ultra60 FE-SEM. Sheet resistance measurements were performed at ambient conditions with a Keithley 2400 source meter instrument, and a conventional 4-point probe station.

3. Results and discussion

3.1. Micro-Raman spectroscopy

Fig. 1 represents the typical Raman spectra obtained for unirradiated graphite oxide and excimer laser-reduced graphite oxide in high vacuum after 32 pulses at ~138 mJ/cm^2. Fig. 1 inset shows GO reduction as a function of the number of laser pulses. The spectra were normalized to the G peak. In the untreated graphite oxide two main peaks were observed, D (1351 cm^{-1}) and G (1590 cm^{-1}). Due to the sp^3 hybridization nature of the graphite oxide carbon bonds, the D peak is very

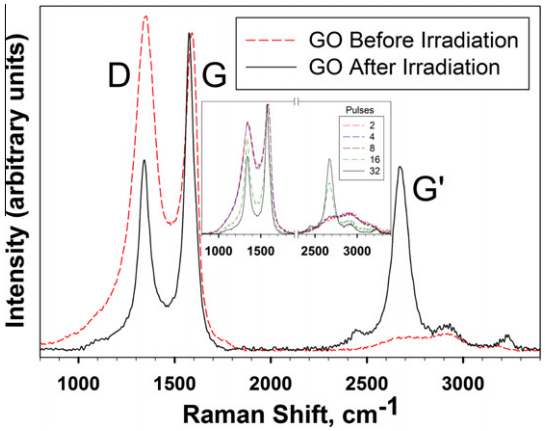

Fig. 1 – Typical Raman spectrum of untreated GO (red curve) compared with a spectrum of excimer laser-reduced GO (black curve) produced with 32 pulses at ~138 mJ/cm^2 laser fluence in high vacuum (~10^{-6} Torr). The inset is the pulse dependence of GO reduction at 138 mJ/cm^2 in high vacuum (~10^{-6} Torr). (For interpretation of the references to color in this figure legend, the reader is referred to the web version of this article.)

prominent. Upon excimer laser irradiation, the D peak position is shifted by 9 cm^{-1} to 1342 cm^{-1} and the intensity is greatly reduced; the G peak position is shifted by 25 cm^{-1} to 1575 cm^{-1} and a prominent G′ peak grows at 2672 cm^{-1} indicating production of graphitic features. This G′ peak can be fit with a single Lorentzian with a typical FWHM between 50–65 cm^{-1} [14]. Previous work has indicated that the G′ peak with a single Lorentzian profile can reveal the presence of turbostratic graphite, which is composed of multiple randomly oriented graphene sheets [24,25]. The presence of the D peak in the laser-reduced graphite oxide spectrum can be attributed either to the remaining oxygen species present after the reduction or possibly to the defects associated with the edge scattering in the graphene sheets. Alternatively, due to the laser reduced layer being directly on top of graphite oxide, the D band can be partially attributed to the Raman scattering from the underlying GO support. Additionally, Raman spectroscopy can be used to estimate the mean domain sizes or interdefect distances (L_a) in graphene from the empirical relationship L_a (nm) = $(2.4\times10^{-10})\lambda_l^4(I_D/I_G)^{-1}$, where λ_l is the probe laser wavelength (nm) and I_D and I_G are the integrated Raman intensities of the D and G bands [26,27]. From Fig. 1, the L_a values of 18.2 nm and 31.5 nm were calculated for the untreated and the laser reduced graphite oxide, respectively. An increase in the L_a value indicates a transition of the laser-reduced graphite oxide to a more ordered state with fewer defects [27].

3.2. *X-ray photoelectron spectroscopy*

XPS is often used as a technique for verifying reduction of graphite oxide. XPS is capable of quantitative measurement of material composition and elucidating the chemical environment surrounding atoms by measuring core level shifts, which are affected by bonding states. Since it is difficult to extract detailed information regarding defects and structure within the graphene lattice, XPS analysis is generally more useful when done in conjunction with Raman spectroscopy. Collectively these two approaches can provide a more definitive verification of graphene formation from GO. Figs. 2 and 3 illustrate the individual XPS spectra of the graphite oxide film before (Figs. 2a and 3a) and after (Figs. 2b and 3b) excimer laser irradiation in vacuum (~10^{-6} Torr) with 32 pulses at ~138 mJ/cm^2. Note this data is only representative of the surface of our samples as the escape depth of X-ray photoelectrons at these energies is on the order of 10 nm. More specifically, we sample the film surface, which includes micron-size domains, but we are not sampling the bulk.

The untreated graphite oxide (Fig. 2a), as expected, has dominant carbon and oxygen features with a trace amount of residual sulfur left over from the synthesis of graphite oxide via the modified Hummers' method. The initial oxygen content is ~29% and the C/O ratio is 2.43 (based on the ratio of areas under the curve of C1s and O1s peaks). Curve fitting of the C1s peak (Fig. 3a) reveals the presence of oxygen containing functionalities in the form of epoxy, hydroxyl and carbonyl groups. Once the laser reduction is performed, a drastic change in the amount of oxygen is observed (Fig. 2b). The oxygen content is decreased to as little as ~2–3%, and the C/O ratio reaches 40. Curve fitting of the C1s peak in the laser-reduced sample (Fig. 3b) confirms a predominance of the sp^2 hybridized carbon, indicating graphene formation; although a contribution from carbonyl peaks is also observed.

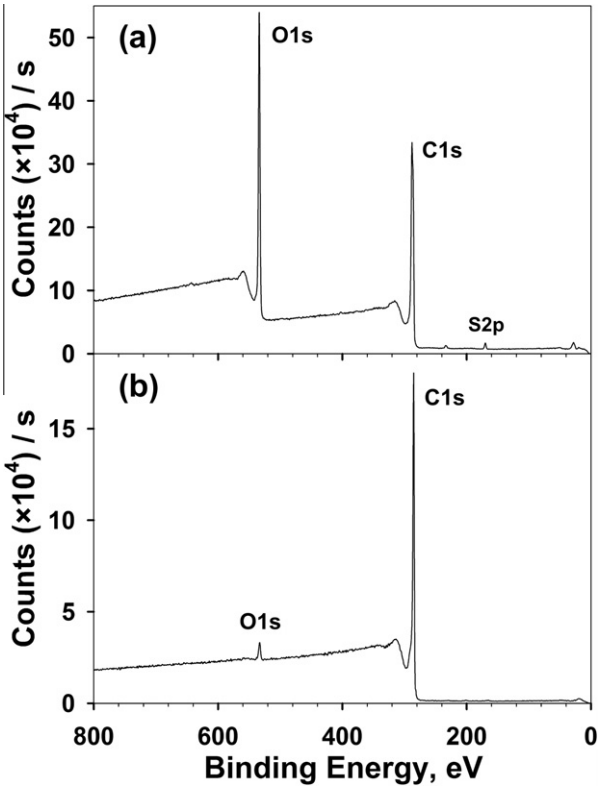

Fig. 2 – XPS spectra of graphite oxide before (a) and after (b) excimer laser irradiation in high vacuum after 32 pulses at ~138 mJ/cm^2 laser fluence. Graphite oxide before irradiation has ~29% oxygen content and a C/O ratio of 2.43. After the excimer laser irradiation, the oxygen content is decreased to ~2–3% and the C/O ratio is increased to 40.

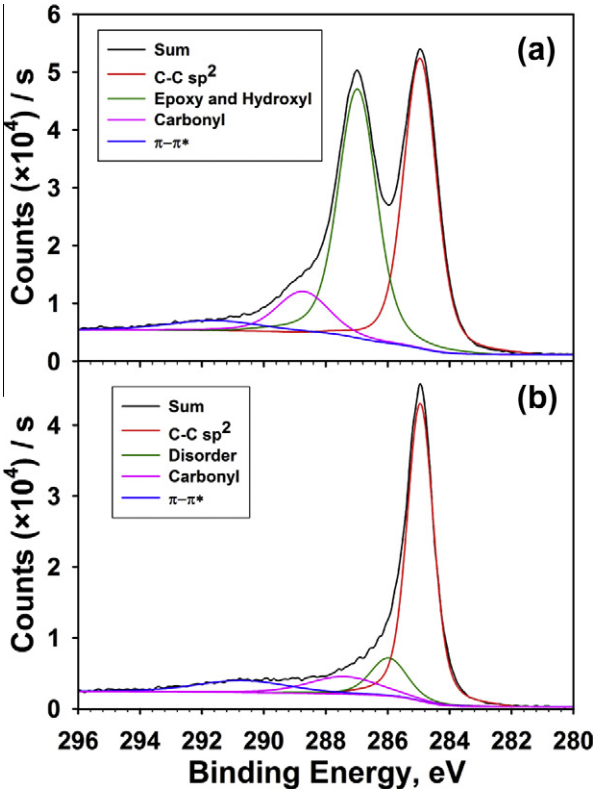

Fig. 3 – XPS C1s peak spectra of graphite oxide before (a) and after (b) excimer laser irradiation in high vacuum with 32 pulses at ~138 mJ/cm^2 laser fluence. Before irradiation, the C1s peak analysis of the untreated graphite oxide reveals the presence of oxygen containing functionalities in the form of epoxy, hydroxyl and carbonyl groups. After laser irradiation, the peaks associated with the oxygen containing functionalities are diminished, and the predominance of the sp^2 hybridized carbon peak (red curve, peak position at 284.9 eV) confirms graphene formation.

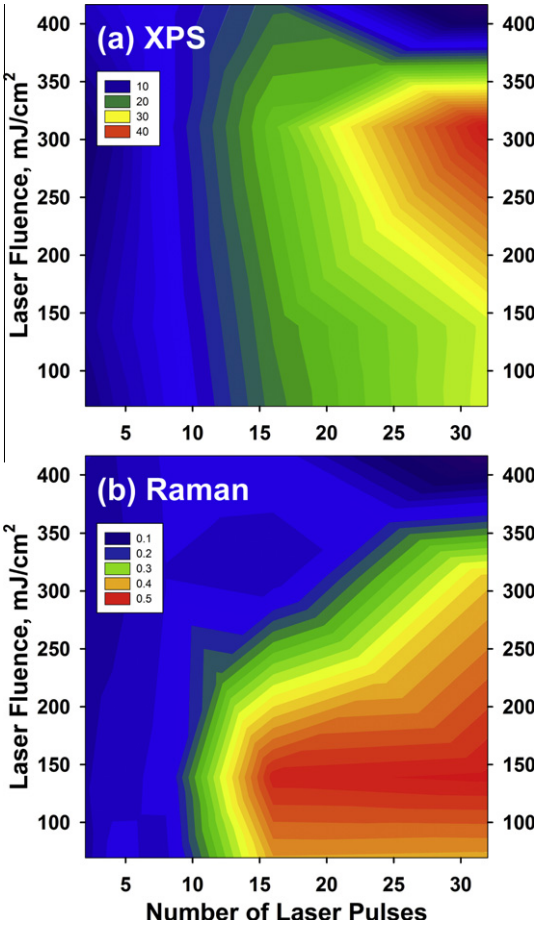

Fig. 4 – 3D plots of the graphite oxide sample after excimer laser reduction in high vacuum as a function of laser fluence and number of laser pulses. (a) Integrated C/O ratios, measured with XPS. (b) G′/G peak intensity ratios, measured with Raman spectroscopy.

3.3. *Laser reduction parameters*

An array of experiments were performed on a GO sample in which the laser fluence was varied from 60 mJ/cm^2 to 400 mJ/cm^2 along one axis, and the number of laser pulses was varied from 2 to 32 along the other axis. Each of the irradiated areas was then analyzed with Raman spectroscopy and XPS, and the data is presented using three dimensional (3D) plots (Figs. 4 and 5). Fig. 4 shows reduction performed in high vacuum (~10^{-6} Torr) and Fig. 5 demonstrates reduction performed in flowing (500 sccm) ultrahigh purity nitrogen. XPS 3D plots (Figs 4a and 5a) were produced from XPS spectra obtained from a ~200 μm area on each of the irradiated spots. The colors in the XPS 3D plots represent different C/O ratios from 2.43 to 40 obtained by taking the ratios of the areas under the C1s and O1s peaks in each spectrum. A higher C/O ratio (red color) means better quality reduction to sp^2 carbon (graphene) features. Also, Raman 3D plots (Figs. 4b and 5b) were produced by obtaining several Raman spectra from each of the laser reduced areas and then averaging them for each of the laser irradiated spots. The colors represent different G′/G peak intensity ratios from 0.1 to 0.5, with the higher ratio (red color) indicating better quality reduction to graphene. It is important to note that the dark blue regions at high laser fluence and high number of laser pulses in Figs. 4 and 5 are due to the GO films being ablated to the point of not having enough material for analysis. Those regions were assigned a value of zero for both the C/O and G′/G ratios.

By observing all four graphs in Figs. 4 and 5, both Raman and XPS show that the application of 10–15 pulses is necessary to initiate laser reduction of graphite oxide to multilayer graphene. This is evident by the transition to higher G′/G ratios and higher C/O ratios (from blue to green in all plots). It is also apparent that XPS is less sensitive than micro-Raman spectroscopy with respect to revealing the irradiated areas with the best graphene quality. Interestingly, a high C/O ratio (from XPS analysis) is not the deciding factor when it comes to determine if graphene signatures are exhibited or not. This is very apparent in the high vacuum reduction plots (Fig. 4a and b) where according to the XPS (Fig. 4a), graphene should be formed after ~30 laser pulses and ~300 mJ/cm^2. Raman

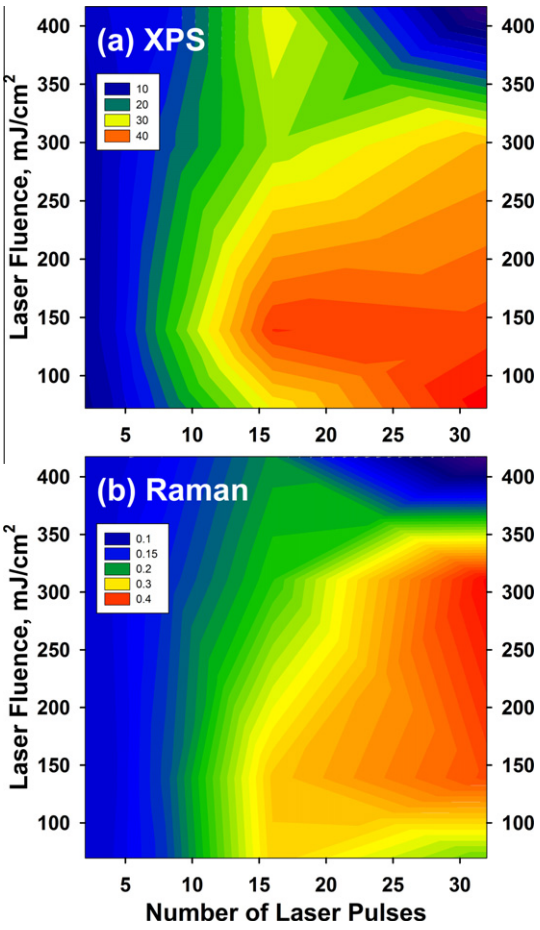

Fig. 5 – 3D plots of the graphite oxide sample after excimer laser reduction in a N_2 environment as a function of laser fluence and number of laser pulses. (a) Integrated C/O ratios, measured with XPS. (b) G'/G peak intensity ratios, measured with Raman spectroscopy.

analysis, however, reveals that high quality graphene signatures are already present after 15–20 laser pulses with only ~150 mJ/cm^2 (Fig. 4b).

When comparing XPS and Raman spectra of GO reduction performed in high vacuum (Fig. 4) with GO reduction performed in nitrogen (Fig. 5), several clear distinctions emerge. According to Raman analysis, ~30 pulses at a fluence of 200–300 mJ/cm^2 are required in nitrogen (Fig. 5b) to achieve a similar level of graphite oxide reduction when compared with that produced by 15–20 laser pulses at ~150 mJ/cm^2 in high vacuum (Fig. 4b). The XPS plots of the C/O ratios for both high vacuum (Fig. 4a) and nitrogen purged samples (Fig. 5a) reveal that, regardless of the environment, a C/O ratio of 40 is reached after irradiation.

3.4. *Mechanisms and plume interactions*

The physics governing laser desorption of semi-conducting and insulating materials can be dominated by electronic and/or thermal processes. The relative contributions of non-thermal vs. thermal processes are governed by the degree of energy localization. Though electron-lattice temperature equilibration occurs on the picosecond time scale in graphite, hole-hole localization, exciton self-trapping and subsequent material ejection can occur. The localization of energy via these pathways can be facilitated by the strain associated with the oxygen in GO [28,29]. It is well known that laser desorption can be initiated by excitation of surface defects and that significant material removal (i.e. ablation) relies upon the production of a critical density of vacancies [30]. These vacancies are mainly created by the localized holes in the top of the valence band and the subsequent hole–hole Coulomb interactions. From XPS and Raman analysis (Figs. 4 and 5), it is clear that an incubation dose of 10–15 shots at ~150 mJ/cm^2 (~2×10^{18} photons/cm^2) is necessary before appreciable laser ablation/reduction can take place. We associate this dose dependence with the formation of vacancies and the removal of terminal O atoms. Indeed, this is consistent with the XPS C/O ratio (~15–20) shown in Figs 4a and 5a. This ratio indicates that an oxygen content of ~4–7% – and the corresponding number of carbon vacancies – is an optimal value to initiate excimer laser reduction of GO to graphene at 248 nm. The samples reduced in high vacuum, with C/O ratio of as low as 25 (Fig. 4a, green color), exhibit graphene features in Raman (Fig. 4b). Though the presence of some residual oxygen functionalities on laser reduced GO is tolerable for preservation of the graphene electronic structure, the best graphene is produced when the reduction is performed in an oxygen-free environment – i.e., vacuum or ultrapure nitrogen. This is evidenced by comparing Raman G'/G peak ratios as a function of environment (see Figs. 4 and 5).

Ejecta formed during laser ablation expand normal to the sample plane in a plume with a shape that is driven by pressure gradients, and therefore is inversely proportional to the beam dimensions. The plume expands initially with a velocity that is determined by the numerous collisions within the very dense collisional Knudsen layer close to the target surface. In vacuum, following the collisions within the Knudsen layer, which result in a fraction of material redeposited on the sample surface, the forward-going component of the plume freely expands. In a background gas, however, this expansion is short-lived – roughly until the pressure within the plume equals that of the surrounding gas. The plume sets in motion a shock wave in the background gas, and a rarefaction wave can lead to further redeposition of material on the target. Under these conditions, it is likely that the difference mentioned above regarding graphene quality as a function of environment may be due to redeposition of the ejected oxidized species and possible reoxidation of the laser reduced GO. This plume behavior is similar to the dynamics reported for the laser ablation of graphite in vacuum and inert gases [31]. Although the composition of the plume during excimer laser reduction of GO has not been analyzed during the present experiment, previous reports of the photoreduction approach [32] and during photon irradiation studies of GO [33,34] show that the plume contains oxygen rich sp^3 hybridized carbon fragments as well as species such as H_2O, CO, O_2 and CO_2. Previous work on laser ablation of carbon and graphite also demonstrates the direct removal of nanoscale graphene sheets [35]. Clustering reactions within the plume can also form higher mass sp^2 hybridized carbon products, and under the N_2 purging conditions utilized in our experiments, these carbon-bearing products can be deposited on the surface and serve as seeds for growth of larger graphene particles or

sheets. Lastly, though the plume may react with the nitrogen gas, no nitrogen incorporation was observed during the XPS analysis of the present samples.

3.5. *SEM analysis, sheet resistance measurements and laser patterning*

Fig. 6a depicts a SEM image of an unirradiated GO sample, showing that it has a smooth surface morphology. Fig. 6b–e shows several views of the GO film after laser processing. After the laser reduction, the film becomes rough with abundant edges, which have a direct effect on the intensity of the D peak in the Raman spectra. It is clear from the SEM images that the surface area of the laser reduced GO is quite large due to the expanded nature of the graphene layers (Fig. 6d,e) with protrusions of reduced graphite oxide as high as ~3.2 μm as seen in the cross sectional view in Fig. 6c. It is interesting to note that the close contact between the laser reduced graphene sheets and the high surface area provide multiple paths for charge transport, and it is likely that the majority of the carriers move through the sheets with little scattering from defects and terminal edges.

To gain insight into carrier transport within this material, sheet resistance under ambient conditions was evaluated as a function of the number of laser pulses (Fig. 7). As mentioned earlier, these samples required larger laser beam spot sizes onto which silver paste contacts could be deposited. These KrF-laser irradiation experiments were carried out in low vacuum (9.8×10^{-2} Torr) with a fluence of ~204 mJ/cm^2. The maximally-reduced Raman spectra obtained from these samples were comparable to those reduced at high vacuum (G′/G of 0.41 vs. 0.50, respectively). The only notable difference is the larger number of laser pulses required for the reduction process, a result which is consistent and predictable from Fig. 4b. The Van der Pauw four-point probe method [36] was utilized, and the lowest sheet resistance measured was ~491 Ω/sq. For GO samples that were pre-reduced thermally at 150 °C for 24 h to decrease the oxygen content from ~29% to ~18%, the lowest sheet resistance measured after laser processing was ~100 Ω/sq. The sheet resistance of untreated GO was previously reported to be ~10^{10} Ω/sq [7], making the present values among the best reported thus far for any laser reduction method. The only other GO reduction approaches that report comparable sheet resistance values are based on the combination of chemical and/or thermal reduction of graphite oxide [4]. It is known that the sheet resistance of GO is related to the C/O ratio [4,5,37–40] and overall film quality/defect density. The very low sheet resistance in our reduced GO can be collectively accounted for by the high C/O ratio, high surface area and many overlapping points of contact.

To demonstrate the applicability of the excimer laser reduction approach, a variety of features have been lithographically patterned on GO samples using laser reduction

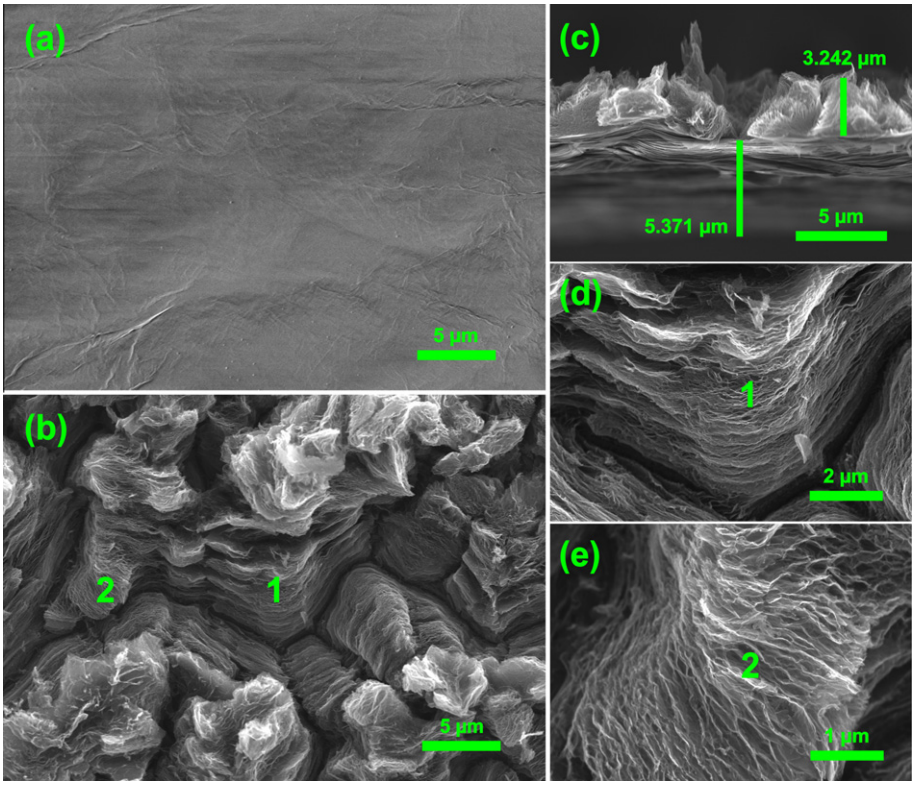

Fig. 6 – Typical SEM images of GO before (a) and after (b–e) excimer laser irradiation in high vacuum with 32 pulses at ~138 mJ/cm^2 laser fluence. (c) The typical cross-sectional view of the excimer laser reduced GO in high vacuum. (d and e) Close-up view of spots 1 and 2 in (b) shows the highly expanded nature of the excimer laser-reduced GO. Note the high surface area and close contact between parts of the reduced GO sheets.

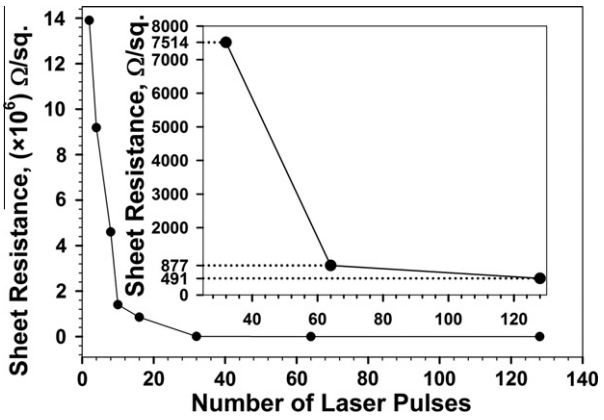

Fig. 7 – Sheet resistance as a function of number of laser pulses, measured from a sample irradiated in vacuum (~9.8×10^{-2} Torr) with a 248 nm KrF excimer laser (fluence of ~204 mJ/cm^2). The inset is the magnified view of the last three data points.

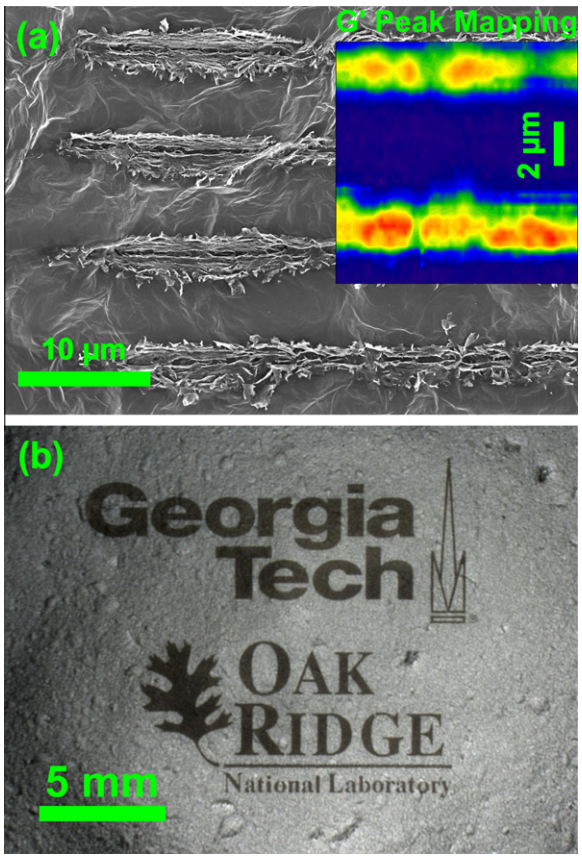

Fig. 8 – (a) Lithographic pattern of microscale parallel lines (~1.5–2 μm wide) produced with a contact mode quartz shadow mask and excimer laser irradiation in high vacuum. The inset is the Raman mapping of the G′ peak at 2672 cm^{-1} as a function of XY position indicating reduction to graphene in the laser irradiated regions. (b) Logos of Georgia Tech and Oak Ridge National Laboratory, produced via contact mode lithography with excimer laser irradiation of graphite-oxide in high vacuum.

at optimal laser fluence and optimal number of laser pulses (Fig. 8). The patterning was performed in contact mode using a quartz shadow mask. The smallest patterned features were ~1.5–2 μm wide as determined by the mask's pattern dimensions. The inset in Fig. 8a shows Raman G′ peak (2672 cm^{-1}) mapping of an area that includes micropatterned lines. The dark blue color represents the areas of unirradiated graphite oxide, whereas the green–yellow–red areas represent the areas with various graphene qualities (red indicating the highest quality). The non-uniformity in quality can be attributed to the use of contact mode instead of projection mode mask lithography. In contact mode, due to the inherent roughness of the GO film, the shadow mask is in intimate contact with some portions of GO and is slightly elevated from others. Also, the shadow mask prevents the escape of the oxygen rich plasma plume produced during laser irradiation, and since it cannot escape, the ejecta redeposits on the laser irradiated areas (as well as the mask). These factors result in material with non-uniform quality. Projection mode lithography should result in more uniform graphene patterning because there is no mask to trap the plume. It is foreseeable that direct patterning of highly conductive nanofeatures [18–20] will be possible because of the short wavelengths produced by excimer lasers. To evaluate the scalability of this method, institutional logos were patterned as shown in Fig. 8b.

4. Conclusions

We have demonstrated excimer laser-induced reduction of graphite oxide using 248 nm photons. The quality of the produced graphene was verified with both Raman and XPS spectroscopies as well as sheet resistance measurements. Specifically, Raman analysis of the excimer laser-reduced samples reveals the formation of a prominent G′ peak at 2672 cm^{-1} and a high G′/G ratio of 0.5. The XPS analysis reveals the C/O ratio to be as high as 40. The sheet resistance was measured to be ~100–500 Ω/sq and these values are among the best reported in the literature for any laser reduction method thus far. The key to complete laser reduction of graphite oxide is pre-treatment with 10–15 pulses at a fluence ~100–300 mJ/cm^2 (i.e. a photon flux of up to 2–4 × 10^{18} photons/cm^2) followed by an additional 10–20 shots. The additional laser shots lead to material removal and laser plume production. This laser-based reduction strategy requires the use of an oxygen free environment. The quality of graphene produced in high vacuum is slightly better than that produced in a N_2 background gas. The use of Raman spectroscopy in conjunction with XPS is essential to verify graphene formation. Scalability of the excimer laser reduction approach was confirmed by patterning institutional logos and microscale features (1.5–2 μm wide parallel lines). Future work will involve further improvements of the process by evaluating the effects of other background gas mixtures on the laser-produced plume composition and dynamics.

Acknowledgements

The authors acknowledge helpful discussions with Dr. Alex Puretzky and support from the Georgia Tech Laboratory for

New Electronic Materials, National Science Foundation Grant: NSF MRSEC DMR-0820382. We thank Prof. Paul Houston for use of the KrF excimer laser at Georgia Institute of Technology. A portion of this research was conducted at the Center for Nanophase Materials Sciences, which is sponsored at Oak Ridge National Laboratory by the Scientific User Facilities Division, Office of Basic Energy Sciences, U.S. Department of Energy.

REFERENCES

[1] Novoselov KS, Geim AK, Morozov SV, Jiang D, Zhang Y, Dubonos SV, et al. Electric field effect in atomically thin carbon films. Science 2004;306(5696):666–9.
[2] Berger C, Song ZM, Li TB, Li XB, Ogbazghi AY, Feng R, et al. Ultrathin epitaxial graphite: 2D electron gas properties and a route toward graphene-based nanoelectronics. J Phys Chem B 2004;108(52):19912–6.
[3] Li XS, Cai WW, An JH, Kim S, Nah J, Yang DX, et al. Large-area synthesis of high-quality and uniform graphene films on copper foils. Science 2009;324(5932):1312–4.
[4] Ghosh T, Biswas C, Oh J, Arabale G, Hwang T, Luong ND, et al. Solution-processed graphite membrane from reassembled graphene oxide. Chem Mater 2012;24(3):594–9.
[5] Becerril HA, Mao J, Liu Z, Stoltenberg RM, Bao Z, Chen Y. Evaluation of solution-processed reduced graphene oxide films as transparent conductors. ACS Nano 2008;2(3):463–70.
[6] Stankovich S, Dikin DA, Piner RD, Kohlhaas KA, Kleinhammes A, Jia Y, et al. Synthesis of graphene-based nanosheets via chemical reduction of exfoliated graphite oxide. Carbon 2007;45(7):1558–65.
[7] Gilje S, Han S, Wang M, Wang KL, Kaner RB. A chemical route to graphene for device applications. Nano Lett 2007;7(11):3394–8.
[8] Cote LJ, Cruz-Silva R, Huang JX. Flash reduction and patterning of graphite oxide and its polymer composite. J Am Chem Soc 2009;131(31):11027–32.
[9] Gilje S, Dubin S, Badakhshan A, Farrar J, Danczyk SA, Kaner RB. Photothermal deoxygenation of graphene oxide for patterning and distributed ignition applications. Adv Mater 2010;22(3):419–23.
[10] Huang L, Liu Y, Ji LC, Xie YQ, Wang T, Shi WZ. Pulsed laser assisted reduction of graphene oxide. Carbon 2011;49(7):2431–6.
[11] Gao W, Singh N, Song L, Liu Z, Reddy ALM, Ci LJ, et al. Direct laser writing of micro-supercapacitors on hydrated graphite oxide films. Nat Nanotechnol 2011;6(8):496–500.
[12] Zhou Y, Bao QL, Varghese B, Tang LAL, Tan CK, Sow CH, et al. Microstructuring of graphene oxide nanosheets using direct laser writing. Adv Mater 2010;22(1):67–71.
[13] Zhang YL, Guo L, Wei S, He YY, Xia H, Chen QD, et al. Direct imprinting of microcircuits on graphene oxides film by femtosecond laser reduction. Nano Today 2010;5(1):15–20.
[14] Sokolov DA, Shepperd KR, Orlando TM. Formation of graphene features from direct laser-induced reduction of graphite oxide. J Phys Chem Lett 2010;1(18):2633–6.
[15] Abdelsayed V, Moussa S, Hassan HM, Aluri HS, Collinson MM, El-Shall MS. Photothermal deoxygenation of graphite oxide with laser excitation in solution and graphene-aided increase in water temperature. J Phys Chem Lett 2010;1(19):2804–9.
[16] Eswaraiah V, Aravind SSJ, Ramaprabhu S. Top down method for synthesis of highly conducting graphene by exfoliation of graphite oxide using focused solar radiation. J Mater Chem 2011;21(19):6800–3.
[17] Wei Z, Wang D, Kim S, Kim S-Y, Hu Y, Yakes MK, et al. Nanoscale tunable reduction of graphene oxide for graphene electronics. Science 2010;328(5984):1373–6.
[18] Brueck SRJ. There are no fundamental limits to optical lithography. In: Guenther AH, editor. International trends in applied optics. SPIE Press; 2002. p. 85–6.
[19] Xia QF, Chou SY. Applications of excimer laser in nanofabrication. Appl Phys A Mater Sci Process 2010;98(1):9–59.
[20] Li L, Hong M, Schmidt M, Zhong M, Malshe A, Huis in't Veld B, et al. Laser nano-manufacturing – state of the art and challenges. CIRP Ann Manuf Technol 2011;60(2):735–55.
[21] Fernández-Merino MJ, Paredes JI, Villar-Rodil S, Guardia L, Solís-Fernández P, Salinas-Torres D, et al. Investigating the influence of surfactants on the stabilization of aqueous reduced graphene oxide dispersions and the characteristics of their composite films. Carbon 2012;50(9):3184–94.
[22] Brodie BC. On the atomic weight of graphite. Philos Trans R Soc Lond 1859;149:249–59.
[23] Hummers WS, Offeman RE. Preparation of graphitic oxide. J Am Chem Soc 1958;80(6):1339.
[24] Malard LM, Pimenta MA, Dresselhaus G, Dresselhaus MS. Raman spectroscopy in graphene. Phys Rep 2009;473(5–6):51–87.
[25] Lenski DR, Fuhrer MS. Raman and optical characterization of multilayer turbostratic graphene grown via chemical vapor deposition. J Appl Phys 2011;110(1):013720–4.
[26] Cancado LG, Takai K, Enoki T, Endo M, Kim YA, Mizusaki H, et al. General equation for the determination of the crystallite size La of nanographite by Raman spectroscopy. Appl Phys Lett 2006;88(16):163106–9.
[27] Ferrari AC. Raman spectroscopy of graphene and graphite: disorder, electron-phonon coupling, doping and nonadiabatic effects. Solid State Commun 2007;143(1–2):47–57.
[28] Zhang H, Miyamoto Y. Graphene production by laser shot on graphene oxide: an ab initio prediction [vol. 85, 033402, 2012]. Phys Rev B 2012;85(8):089901E.
[29] Zhang H, Miyamoto Y. Graphene production by laser shot on graphene oxide: an ab initio prediction. Phys Rev B 2012;85(3):033402–6.
[30] Itoh N, Stoneham AM. Materials modification by electronic excitation. Radiat Eff Defects Solids 2001;155(1–4):277–90.
[31] Puretzky AA, Geohegan DB, Haufler RE, Hettich RL, Zheng XY, Compton RN. Laser-ablation of graphite in different buffer gases. In: Miller JC, Geohegan DB, editors. Laser Ablation: Mechanisms and Applications - II. Woodbury: AIP Press; 1994. p. 365–74.
[32] Shulga YM, Martynenko VM, Muradyan VE, Baskakov SA, Smirnov VA, Gutsev GL. Gaseous products of thermo- and photo-reduction of graphite oxide. Chem Phys Lett 2010;498(4–6):287–91.
[33] Kong X, Huang Y, Chen Y. Difference in formation of carbon cluster cations by laser ablation of graphene and graphene oxide. J Mass Spectrom 2012;47(4):523–8.
[34] Kong XL, Li SQ, Zhang S, Huang Y, Cheng YS. Large carbon cluster anions generated by laser ablation of graphene. J Am Soc Mass Spectrom 2011;22(11):2033–41.
[35] Lenner M, Kaplan A, Huchon C, Palmer RE. Ultrafast laser ablation of graphite. Phys Rev B 2009;79(18):184105–16.
[36] Van der Pauw LJ. A method of measuring specific resistivity and Hall effect of discs of arbitrary shape. Philips Res Rep 1958;13(1):1–9.
[37] Eda G, Fanchini G, Chhowalla M. Large-area ultrathin films of reduced graphene oxide as a transparent and flexible electronic material. Nat Nanotechnol 2008;3(5):270–4.

[38] Park S, An J, Piner RD, Jung I, Yang D, Velamakanni A, et al. Aqueous suspension and characterization of chemically modified graphene sheets. Chem Mater 2008;20(21):6592–4.
[39] Shin H-J, Kim KK, Benayad A, Yoon S-M, Park HK, Jung I-S, et al. Efficient reduction of graphite oxide by sodium borohydride and its effect on electrical conductance. Adv Funct Mater 2009;19(12):1987–92.
[40] Sreeprasad TS, Samal AK, Pradeep T. Tellurium nanowire-induced room temperature conversion of graphite oxide to leaf-like graphenic structures. J Phys Chem C 2009;113(5):1727–37.